



Supplement of

Characterization of biogenic volatile organic compounds and their oxidation products in a stressed spruce-dominated forest close to a biogas power plant

Junwei Song et al.

Correspondence to: Junwei Song (junwei.song@ircelyon.univ-lyon1.fr) and Harald Saathoff (harald.saathoff@kit.edu)

The copyright of individual parts of the supplement might differ from the article licence.

1 Supplement

2 S1. Data processing of CHARON-PTR-ToF-MS

3 The raw data files of CHARON-PTR-ToF-MS were processed by the Ionicon Data Analyzer
4 (IDA 1.0.2, Ionicon Analytik). Mass calibrations were performed using four ion peaks including
5 H_3O^+ (m/z 21.022), $\text{C}_3\text{H}_6\text{OH}^+$ (m/z 59.049), $\text{C}_6\text{H}_5\text{I}^+$ (m/z 203.943) and $\text{C}_6\text{H}_5\text{I}_2^+$ (m/z 330.848),
6 where $\text{C}_6\text{H}_5\text{I}^+$ and $\text{C}_6\text{H}_5\text{I}_2^+$ were produced from the internal standard diiodobenzene (Ionicon
7 Analytik). High-resolution peak fitting for each ion was performed automatically by the IDA
8 software and refined manually according to the PTR-ToF-MS literature (Pagonis et al., 2019;
9 Yáñez-Serrano et al., 2021). The quantification procedure of CHARON-PTR-ToF-MS data has
10 been described in detail by (Müller et al., 2017; Leglise et al., 2019). The collision rate (k) between
11 the analyte molecules and PTR reagent ions (H_3O^+) is calculated based on the parametrization
12 method (Su and Chesnavich, 1982; Gioumoussis and Stevenson, 1958; Bosque and Sales, 2002).
13 This method uses the properties of the analyte molecule as input parameters: (i) its molecular
14 weight, (ii) its molecular polarizability which is calculated from the elemental composition using
15 the parametrization method and (iii) its dipole moment which is assumed to be 0.3 and 2.75 D for
16 pure and substituted hydrocarbons, respectively. Assuming no interference of fragmentation, the
17 maximum uncertainty of this quantification method is $\pm 40\%$. The separation of gas and particle
18 measurement data as well as particle background subtractions were performed with the custom-in
19 MATLAB script in IDA. Since the PTR-MS shows slow responses to some organic species
20 especially oxidized species in the particle phase (Piel et al., 2021), the initial 290 s particle-phase
21 data at each CHARON measurement mode were excluded. We also excluded the last 10 s particle-
22 phase data at each CHARON measurement mode to avoid any interference from the switching
23 between different measurement modes. Then the rest of 5 min (300 s) particle data were corrected
24 by the interpolate subtraction of HEPA filter background. An average enrichment factor of ~ 6 was
25 used for calculating the mass concentrations of particles measured by the CHARON based on the
26 CHARON calibration with ammonium nitrate particles (**Fig. S3**) and the ambient measurements
27 of particle size distribution by the NanoScan SMPS (**Fig. S8**). For the gas phase data, we also
28 excluded the initial 290 s and the last 10 s data at each VOC measurement mode, which could
29 minimize the effect of fluctuated drift tube temperature on instrumental sensitivities during first
30 measurement stage (**Fig. S2a**). Then the rest of 5 min (300 s) gas data were corrected by the

31 background subtraction from the measurement of VOC-free synthetic air. Finally, we averaged the
32 background-corrected data in gas and particle phases into 5 min presented in this study.

33 It is well-known that the PTR-MS suffers the ionic fragmentation during the protonation
34 processes (Yuan et al., 2017). According to gas calibrations, the residual fractions were
35 characterized on average $\sim 35\% \pm 2\%$ and $\sim 37\% \pm 2\%$ for protonated isoprene ($C_5H_9^+$, $m/z69.07$)
36 and monoterpenes ($C_{10}H_{17}^+$, $m/z137.13$) respectively after their fragmentation within the
37 CHARON-PTR-ToF-MS. A previous study has found that the fragmentation of 2-methyl-3-buten-
38 2-ol (MBO, $C_5H_{11}O^+$) emitted from biogenic sources inside PTR instruments had interferences on
39 the quantification of isoprene based on the $C_5H_9^+$ signals (Karl et al., 2012). As shown in **Fig. S15**,
40 the concentrations of $C_5H_9^+$ were much higher those of $C_5H_{11}O^+$ in both CHARON-PTR-ToF-MS
41 and Vocus-PTR-ToF-MS, and both ions correlated fairly and poorly with each other ($r= 0.54$ and
42 0.09). It indicates that the fragmentation of MBO have no significant influence on the attribution
43 of $C_5H_9^+$ to isoprene in this study. Recent studies have found that PTR-measured $C_5H_9^+$ signals can
44 be significantly contributed by the fragmentation of cycloalkanes and long-chain aldehydes (e.g.,
45 octanal and nonanal) emitted from anthropogenic sources such as fossil fuel use and cooking in
46 urban regions (Pfanterstill et al., 2023; Coggon et al., 2024). In this study, the concentrations of
47 cycloalkanes and long-chain aldehydes such as octanal ($C_8H_{17}O^+$) and nonanal ($C_9H_{19}O^+$) were two
48 orders of magnitude lower than that of $C_5H_9^+$, thus their interferences were also negligible in this
49 study. Finally, we scaled the measured data of $C_5H_9^+$ and $C_{10}H_{17}^+$ by a factor of 2.86 and 2.70
50 respectively to quantify the concentrations of isoprene and monoterpenes in this study. For other
51 calibrated species including benzene, toluene, xylenes, trimethylbenzene, methanol and acetone,
52 they have minor fragmentation in CHARON-PTR-ToF-MS. Besides, no fragmentation correction
53 was made for uncalibrated VOC species.

54

55 **S2. Comparisons of VOCs between CHARON-PTR-ToF-MS and Vocus-PTR-ToF-MS**

56 With the Vocus-PTR-ToF-MS measurement, 287 VOC ion peaks within the mass range of m/z
57 40–445 were quantified after background correction. Following selection, 157 VOC ion peaks with
58 assigned chemical formulas (primarily mainly $C_xH_y^+$ and $C_xH_yO_z^+$) were used for PMF analysis.
59 For the CHARON-PTR-ToF-MS measurement, 939 ion peaks were automatically identified using
60 the IDA software, and 388 of these ions were assigned with chemical formulas (mainly $C_xH_y^+$ and

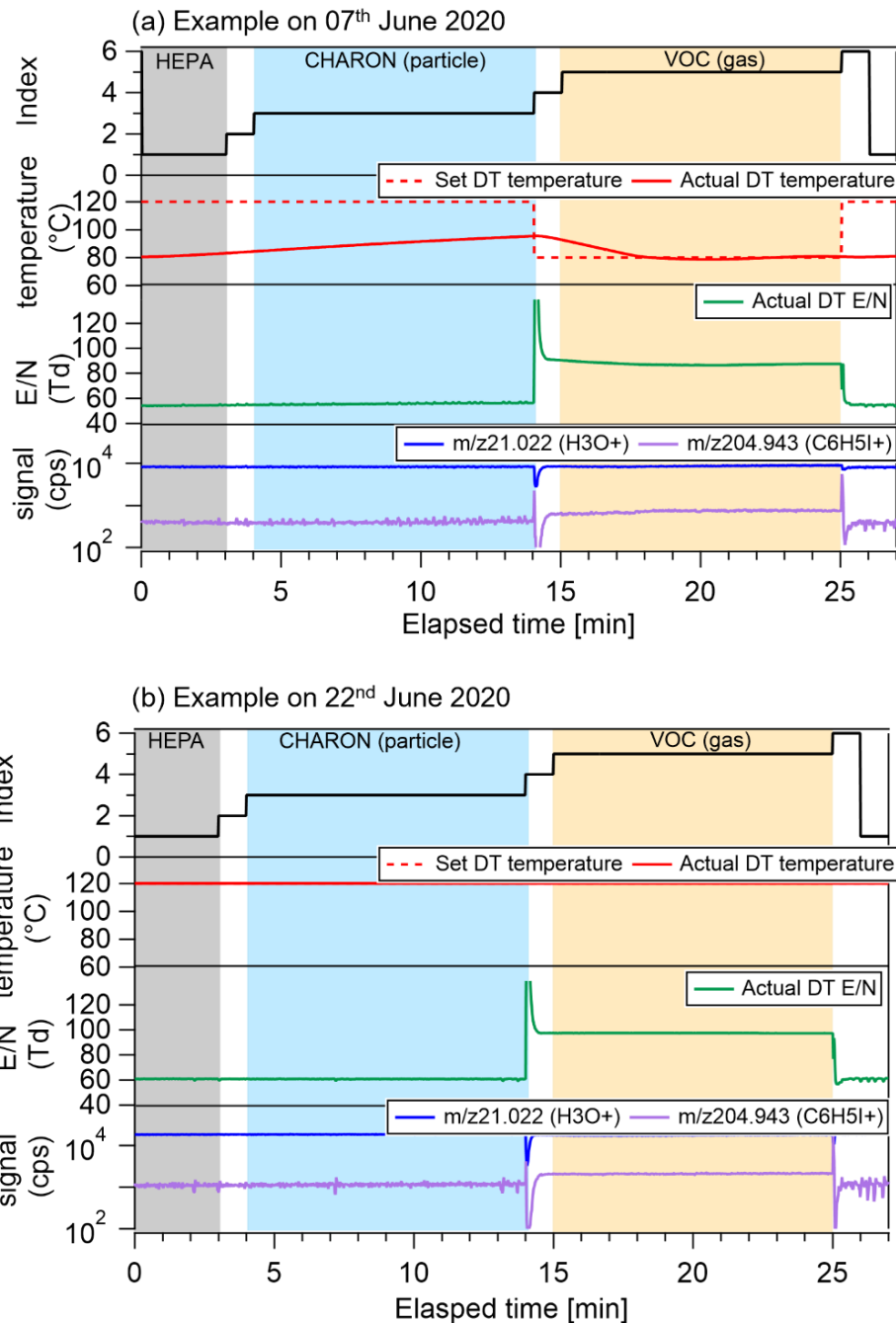
61 $C_xH_yO_z^+$). After background correction, 112 VOC ions measured by the CHARON-PTR-ToF-MS
62 were considered for comparison with those simultaneously measured by the Vocus-PTR-ToF-MS.
63 We first compared the calibrated VOC species measured by the PTR-MS instruments during the
64 entire measurement campaign. As shown in **Fig. S12**, good agreements were observed for $C_6H_7^+$
65 (benzene), $C_7H_9^+$ (toluene), $C_8H_{11}^+$ (C_8 -aromatics) and $C_9H_{13}^+$ (C_9 -aromatics) between CHARON-
66 PTR-MS and Vocus-PTR-MS within the differences of 10-30%. It should be noted that $C_5H_9^+$
67 (isoprene) and $C_{10}H_{17}^+$ (monoterpenes) were fragmented differently inside CHARON-PTR-ToF-
68 MS and Vocus-PTR-ToF-MS. To take account into fragmentation corrections, we scaled the
69 signals of $C_5H_9^+$ and $C_{10}H_{17}^+$ measured by the CHARON-PTR-ToF-MS with a factor of 2.86 and
70 2.70 to obtain the concentrations of isoprene and monoterpenes respectively. Similarly, we scaled
71 the signals of $C_5H_9^+$ and $C_{10}H_{17}^+$ measured by the Vocus-PTR-ToF-MS with a factor of 1.25 and
72 1.67 to obtain the concentrations of isoprene and monoterpenes respectively. Then good
73 agreements were observed for isoprene and monoterpenes between CHARON-PTR-ToF-MS and
74 Vocus-PTR-ToF-MS (**Fig. S12**). We found that $C_3H_7O^+$ (acetone + propanal) measured by
75 CHARON-PTR-ToF-MS were higher than that measured by Vocus- PTR-ToF-MS by a factor of
76 ~ 2.5 . The differences of $C_3H_7O^+$ could be due to PTR-MS fragmentation of higher-molecular-
77 weight VOCs that produce signals at the ion mass of $C_3H_7O^+$ or differences in the detection of
78 acetone and propanal from the two PTR-MS instruments. Besides, the Vocus-PTR-ToF-MS cannot
79 quantify the concentration of methanol (CH_5O^+) due to reduced ion transmission at lower masses
80 ($m/z < 40$), thus no comparison was made.

81 We also summarized the comparisons of a suite of VOC ions measured by Vocus- PTR-ToF-
82 MS and CHARON- PTR-ToF-MS during the second measurement stage (22nd-30th June) in **Table**
83 **S4**. More than 75 VOC ions measured by these two PTR-MS instruments showed good correlations
84 ($r > 0.5$). However, the concentrations of these well-correlated VOC ions measured by Vocus-
85 PTR-ToF-MS were generally higher than those measured by CHARON- PTR-ToF-MS by factors
86 of 1-10. Note that the total concentrations of major VOC ions measured by the CHARON-PTR-
87 ToF-MS and the Vocus-PTR-ToF-MS were comparable (**Fig. S4**). Therefore, the differences for
88 individual VOC species could result from the different sensitivities of each VOC species or
89 fragmentation patterns between these two instruments. In addition, we employed different
90 calculation method for the CHARON-PTR-ToF-MS data and the Vocus-PTR-ToF-MS data, which
91 introduced external differences for the comparison of uncalibrated VOC ions.

92 During the first measurement stage, many VOCs detected by CHARON-PTR-ToF-MS also
93 correlated with those measured by Vocus-PTR-ToF-MS. However, the actual PTR-MS drift tube
94 temperatures were different between the first and second measurement stage, which leads to the
95 disagreement of VOC concentrations over the entire campaign. Here we adopted a simple method
96 to scale the concentrations of selected VOC ions during the first measurement stage. Specifically,
97 the selected VOC ions measured by CHARON- PTR-ToF-MS have good correlations with those
98 measured by Vocus-PTR-ToF-MS during both measurement stages. Then we scaled the
99 concentrations of each selected VOC ions based on the slope differences of first measurement stage
100 to second one. This simple correction method was validated with the calibrated VOC species (**Fig.**
101 **S12**) and useful for other uncalibrated VOC species like oxygenated VOCs and green leaf volatiles
102 (GLV) species (**Figs. S13 and S14**). Therefore, we can present a consistent VOC data set measured
103 by CHARON-PTR-ToF-MS for the entire campaign.

104

105

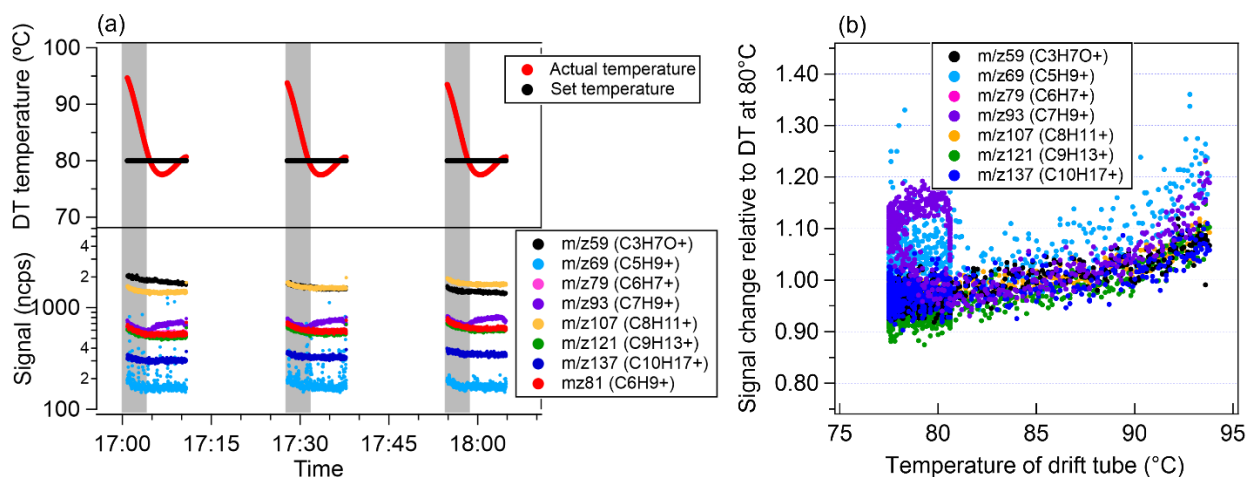


106
 107 **Figure S1.** Examples of alternatingly measurement cycle in the CHARON-PTR-ToF-MS on (a)
 108 7th of June and (b) 22nd of June 2020. Time series of PTR mode index, set and actual PTR drift tube
 109 (DT) temperature, actual DT E/N value, reagent ion (H₃O⁺) and mass calibration ion (C₆H₅I⁺) for
 110 the examples.

111

112

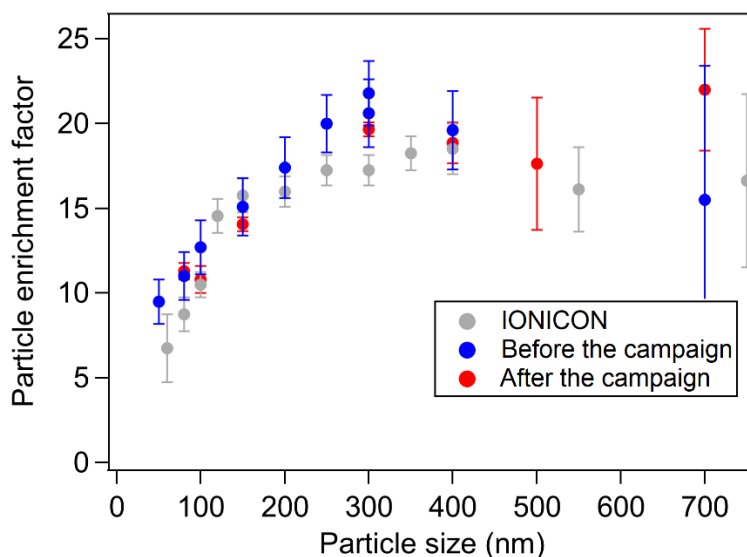
113



114

115 **Figure S2.** Three alternatingly measurement cycles for the ~100 times diluted IONICON gas
116 cylinder by the CHARON-PTR-ToF-MS with the same setting during first measurement stage (5th-
117 19th of June 2020) of field campaign. (a) Time series of set and actual PTR drift tube (DT)
118 temperature and the normalized calibrated VOC signals. The grey shaded areas mark the first 4
119 minutes when the actual DT temperature was rapidly changed back to ~80 °C. (b) Signal change
120 of VOCs relative to those measured with DT temperature at 80 °C.

121

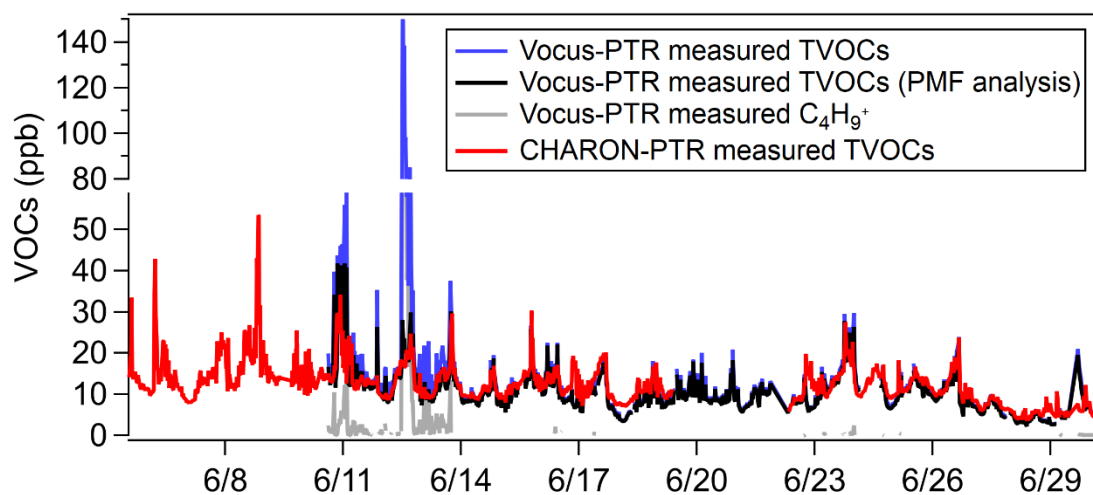


122

123 **Figure S3.** CHARON inlet calibrated enrichment factor of ammonium nitrate as a function of
124 particle size in the 60-700 nm range before and after the measurement campaign in comparison to
125 the enrichment factor certified by the IONICON.

126

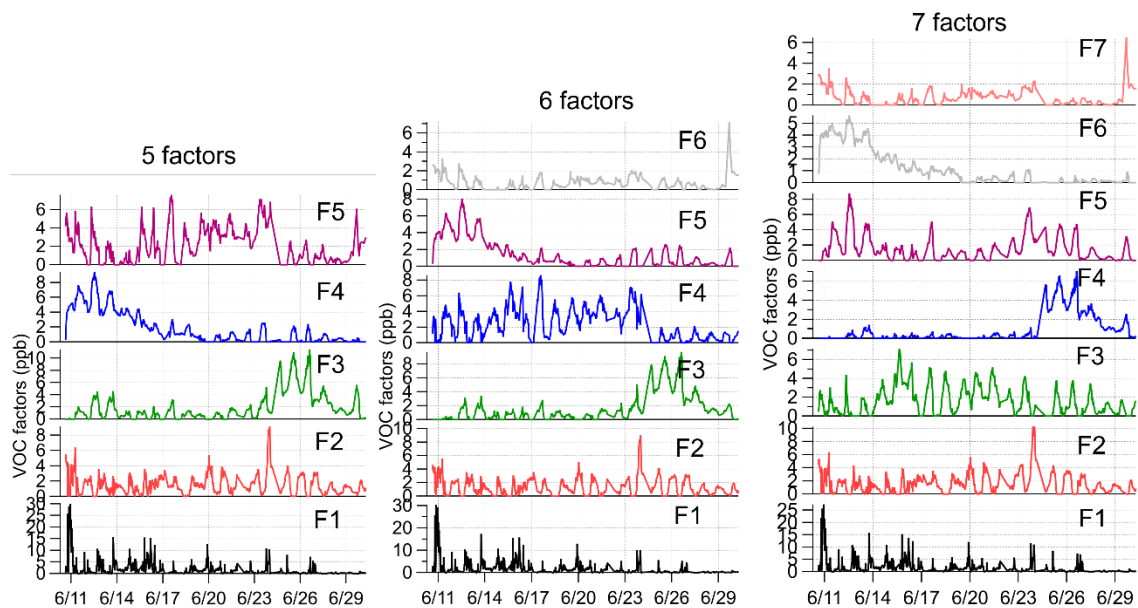
127



128

129 **Figure S4.** Time series of mixing ratios of 287 VOCs (blue), 157 VOCs ions for the PMF analysis
130 (black) and C₄H₉⁺ that was measured by the Vocus-PTR-ToF-MS. The total mixing ratios of 112
131 major VOC ions measured by the CHARON-PTR-ToF-MS (red) is shown for comparison.

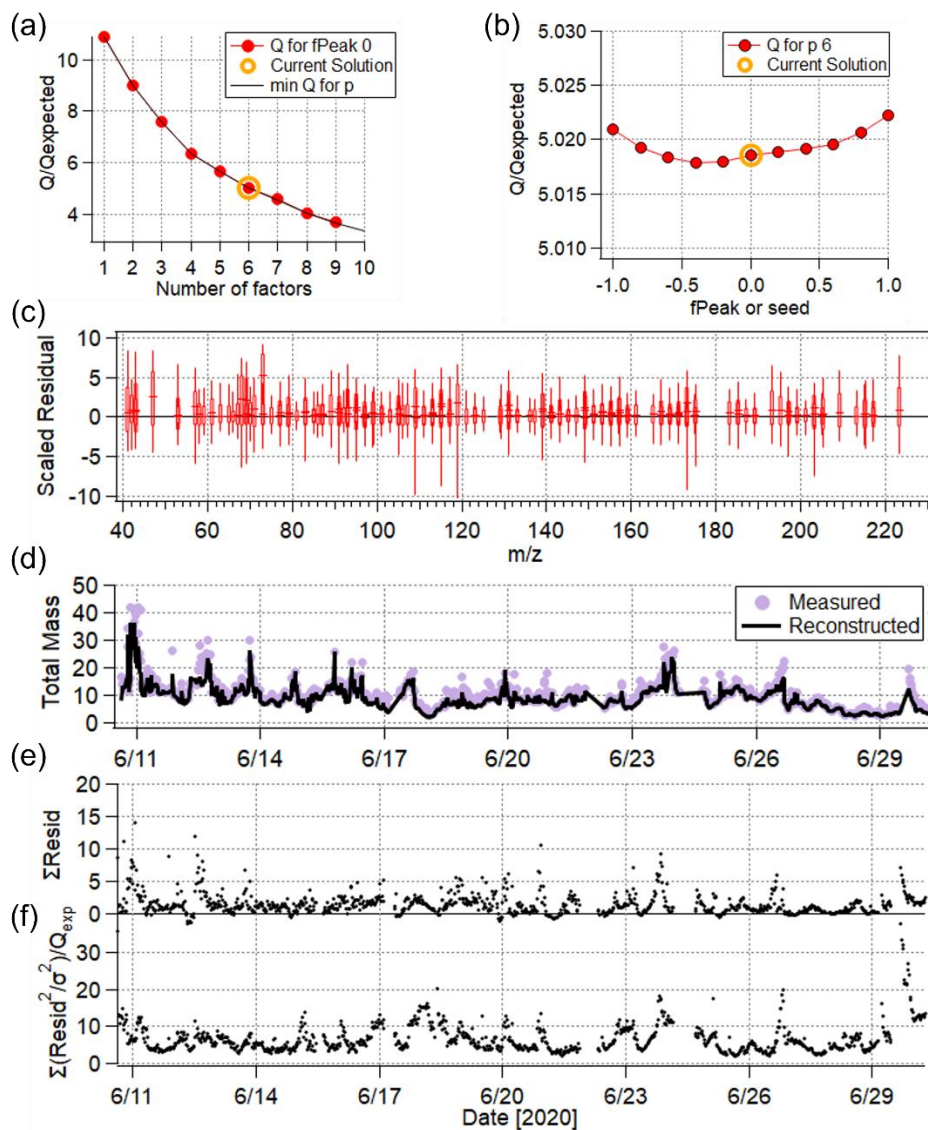
132



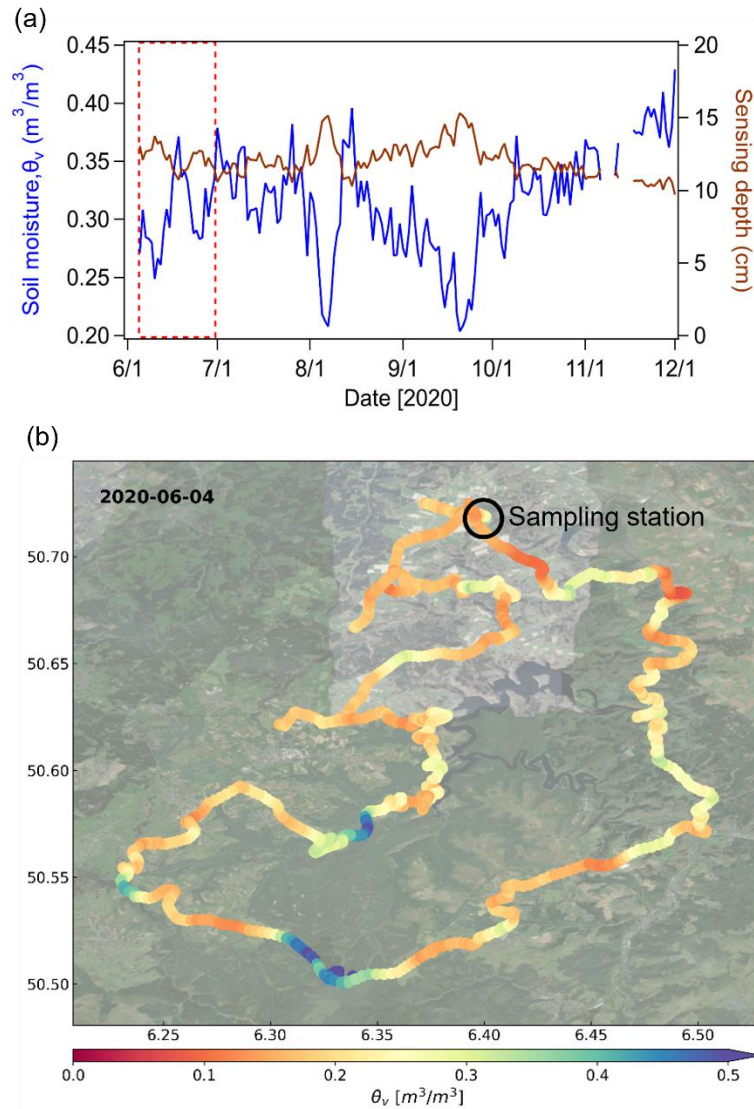
133

134 **Figure S5.** Time series for 5-7 VOC factors resolved from the PMF analysis of Vocus-PTR-ToF-
 135 MS data. Compared to the 5-factor solution, a new factor F6 was resolved in the 6-factor solution.
 136 Further increasing factor number to 7 only led to the factor splitting, resulting in uninterpretable
 137 factor time series.

138

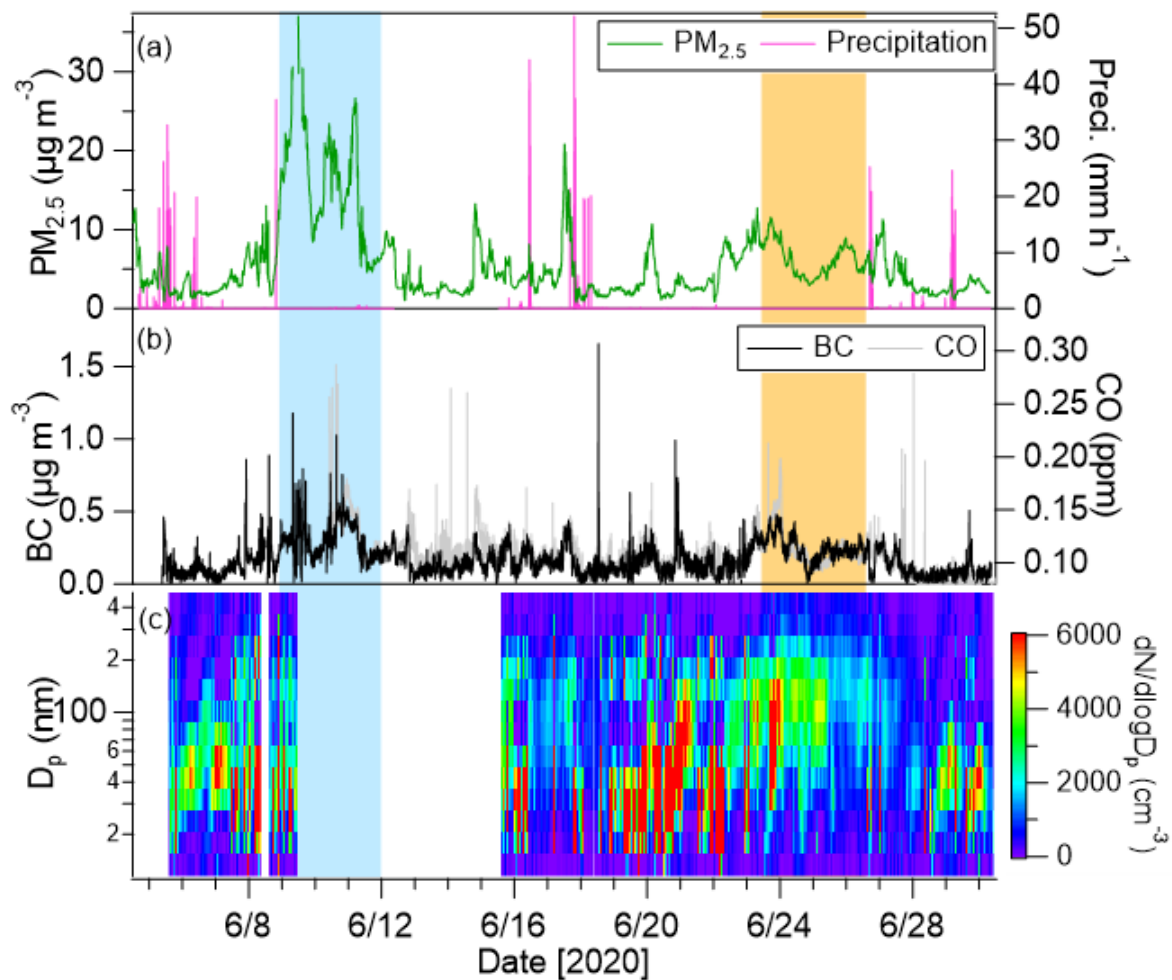


139
 140 **Figure S6.** A summary of diagnostic plots for the PMF analysis of Vocus-PTR-ToF-MS mass
 141 spectral data: (a) Q/Q_{exp} as a function of number of factors; (b) Q/Q_{exp} as a function of f_{peak} or
 142 seed values; (c) scaled residual for each VOC ion; (d) comparison of measured and PMF
 143 reconstructed mass; (e-f) time series of residual and Q/Q_{exp} values.

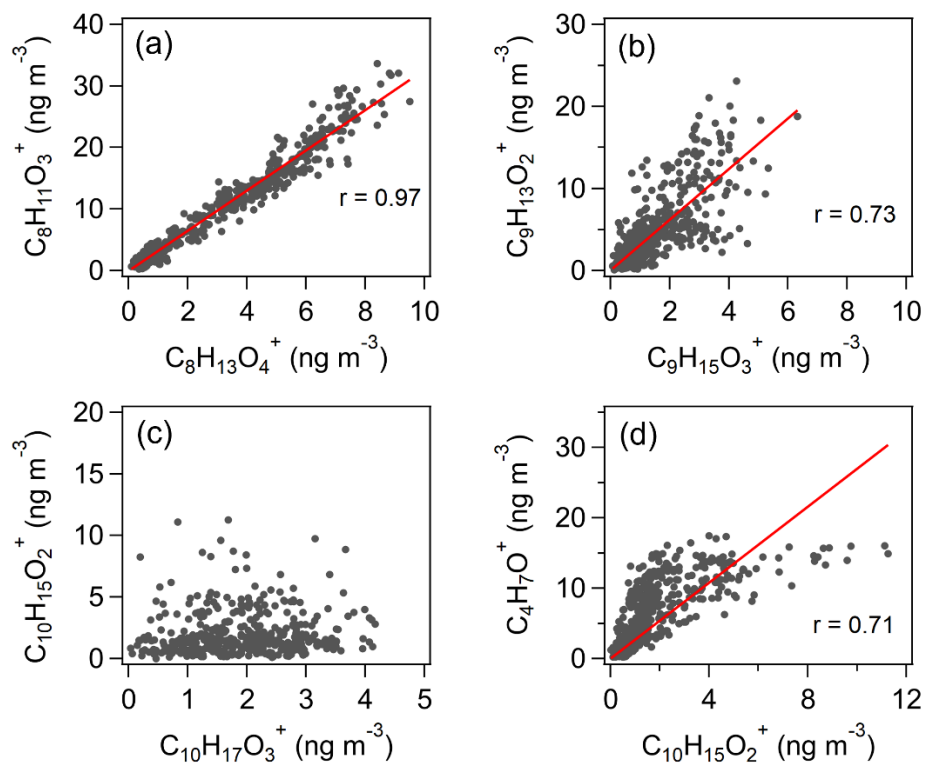


144

145 **Figure S7.** (a) Time series of daily soil moisture (θ_v) and sensing depth measured by a cosmic
 146 ray neutron sensor (CRNS) which was located ~ 150 m southwest of our sampling site. The red
 147 dashed box shows the concurrent sampling period at our measurement container during 5th-30th
 148 June 2020; (b) Spatial distribution of soil moisture in the northern Eifel derived from the
 149 measurement by a CRNS rover during 4th June 2020 (©Google Earth). The black circle shows
 150 the location of the sampling container.



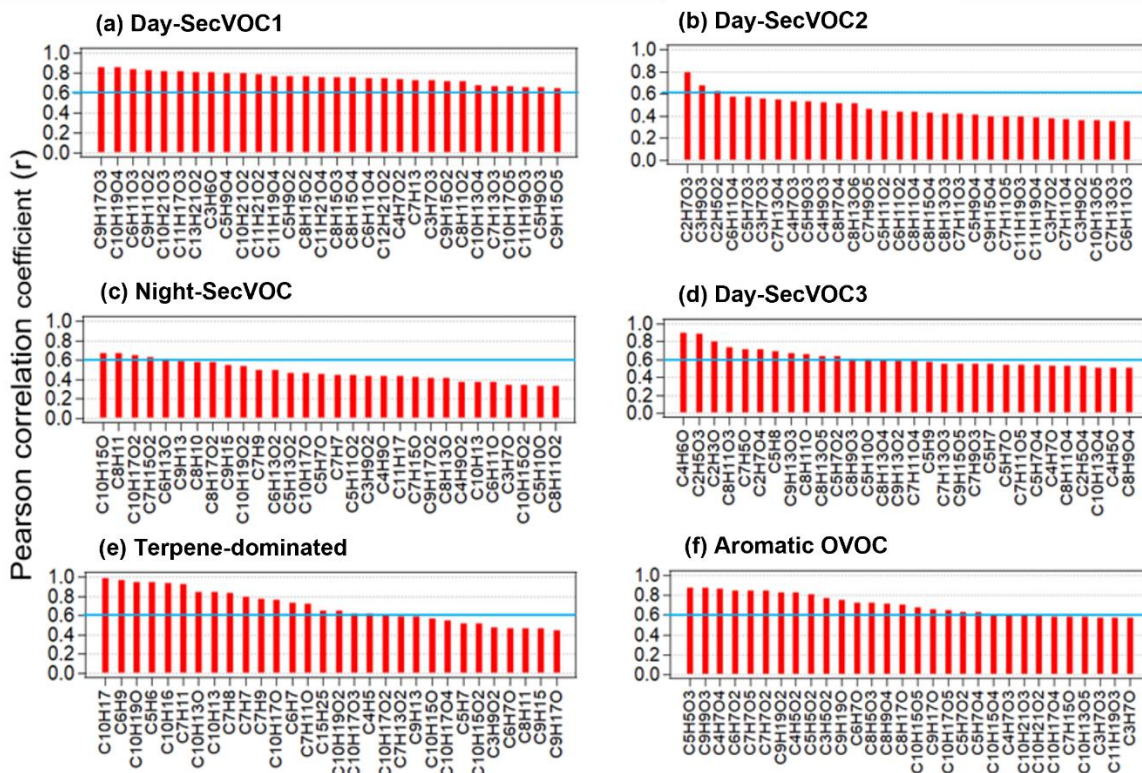
151
 152 **Figure S8.** Time series of (a) $\text{PM}_{2.5}$ mass concentrations and precipitation, (b) BC mass
 153 concentrations and CO. (c) particle number size distributions measured by the NanoScan SMPS.
 154 The blue and yellow shaded areas mark low-T and high-T episodes.



155
 156 **Figure S9.** Scatter plots of parent ions and their potential fragment ions: (a) $\text{C}_8\text{H}_{13}\text{O}_4^+$ (norpinic
 157 acid and its isomers) vs. $\text{C}_8\text{H}_{11}\text{O}_3^+$; (b) $\text{C}_9\text{H}_{15}\text{O}_3^+$ (norpinonic acid and its isomers) vs. $\text{C}_9\text{H}_{13}\text{O}_2^+$
 158 and (c-d) $\text{C}_{10}\text{H}_{17}\text{O}_3^+$ (cis-pinonic acid and its isomers) vs. $\text{C}_{10}\text{H}_{15}\text{O}_2^+$ and $\text{C}_{10}\text{H}_{15}\text{O}_2^+$ vs. $\text{C}_4\text{H}_7\text{O}^+$.

159

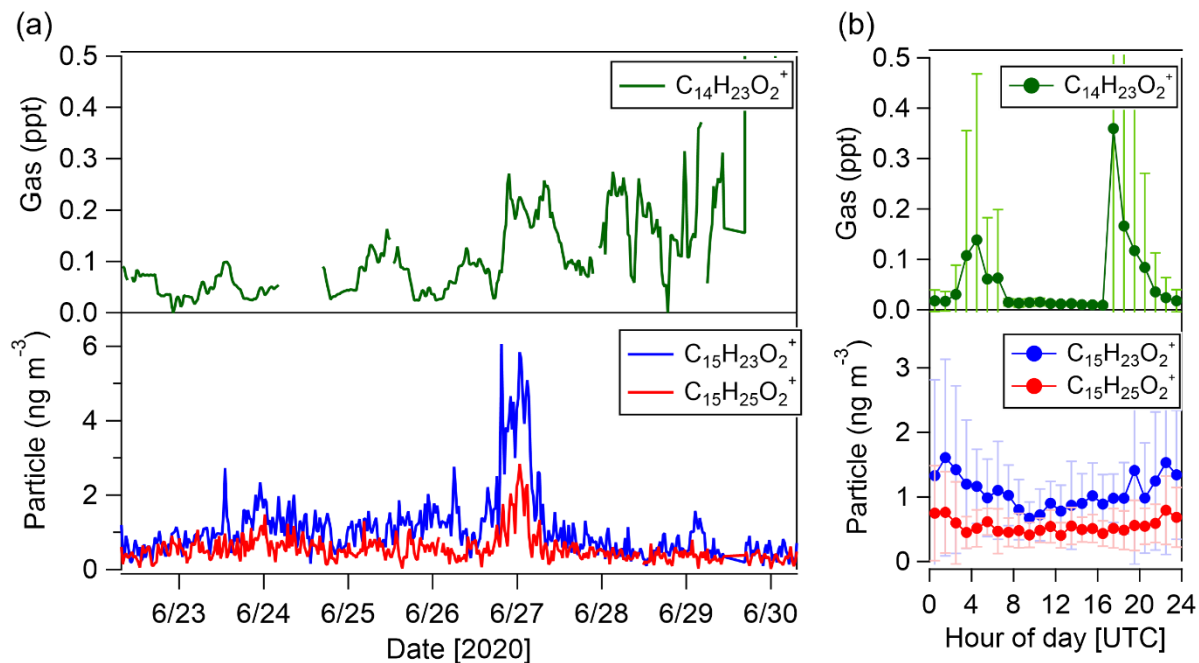
160



161
 162 **Figure S10.** Results of the correlation analysis of six VOC factors resolved from the PMF analysis
 163 of Vocus-PTR-ToF-MS mass spectral data with all VOC ions sorting by correlation coefficient.
 164 The blue lines mark at $r = 0.6$ to indicate relatively good correlations.

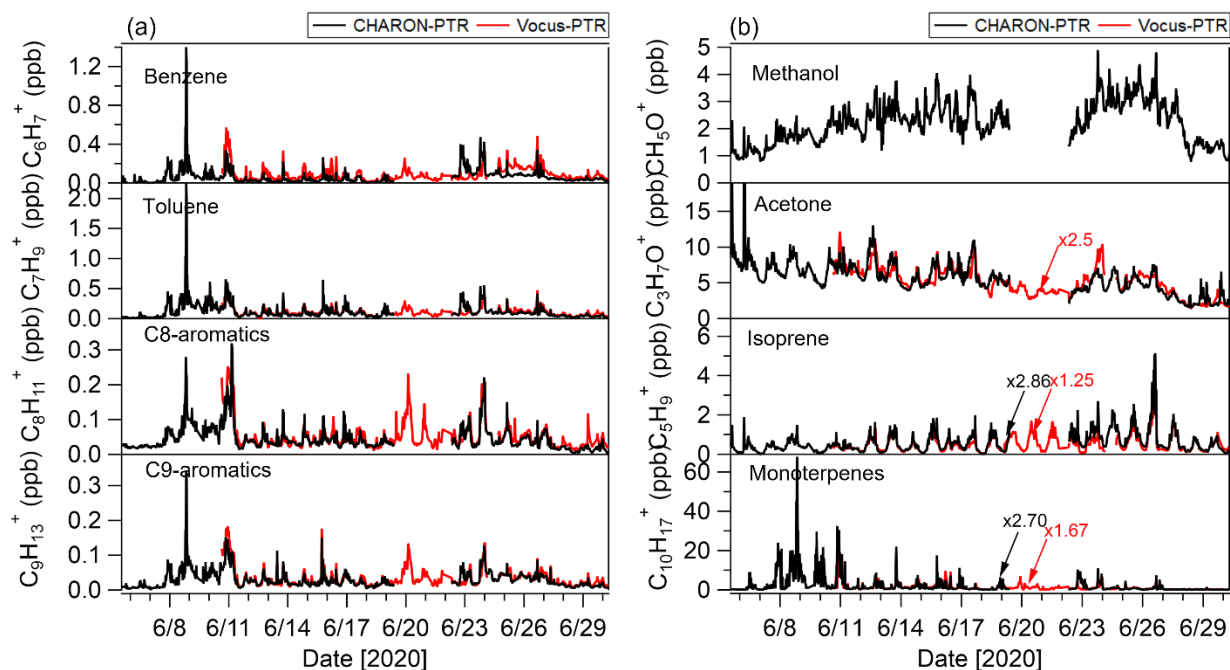
165

166



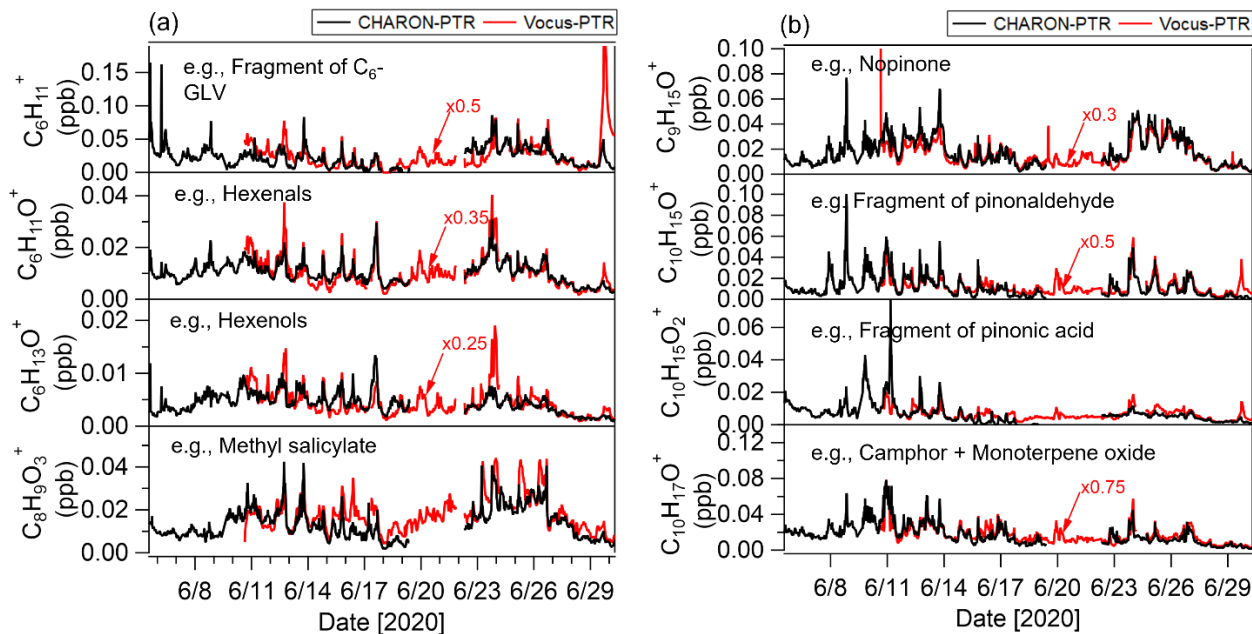
167
 168 **Figure S11.** Time series of sesquiterpene oxidation products (a) $C_{14}H_{23}O_2^+$ in gas phase measured
 169 by the Vocus-PTR-ToF-MS and $C_{15}H_{23}O_2^+$ and $C_{15}H_{25}O_2^+$ in particle phase measured by the
 170 CHARON-PTR-ToF-MS, and (b) their diurnal variations.

171
 172
 173
 174
 175
 176

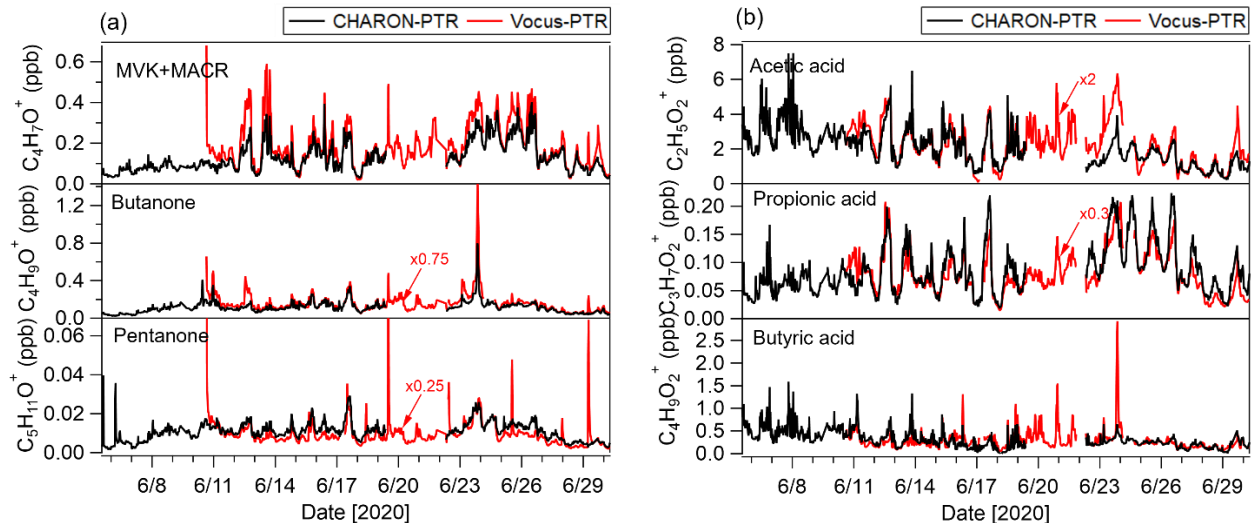


177
 178 **Figure S12.** Comparisons of VOCs measured by CHARON-PTR-ToF-MS and Vocus-PTR-ToF-
 179 MS: (a) aromatic hydrocarbons, (b) methanol, acetone, isoprene and monoterpenes. The data of
 180 $C_5H_9^+$ and $C_{10}H_{17}^+$ were scaled to obtain the concentrations of isoprene and monoterpenes based
 181 on their fragmentation patterns in CHARON-PTR-ToF-MS and Vocus-PTR-ToF-MS.

182

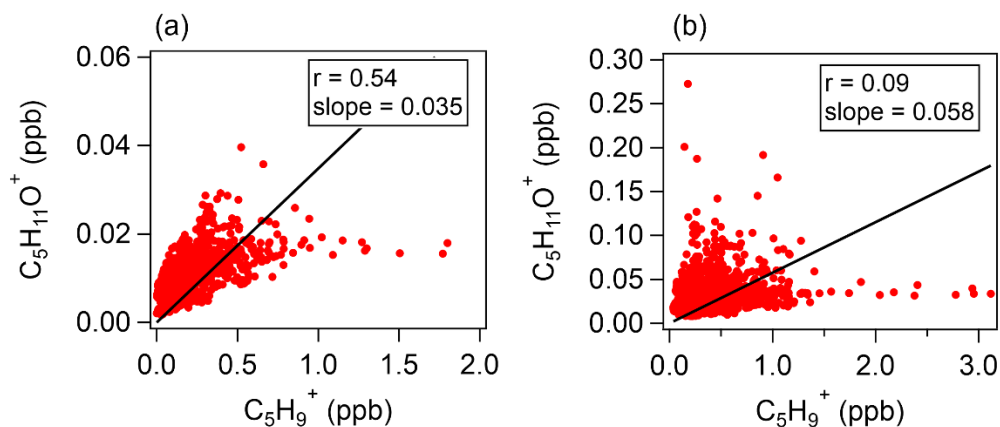


183
 184 **Figure S13.** Comparisons of VOCs measured by CHARON-PTR-ToF-MS and Vocus-PTR-ToF-
 185 MS: (a) VOC ions related to green leaf volatiles (GLV), (b) VOC ions related to monoterpene
 186 oxidation products. The Vocus-PTR-ToF-MS data was scaled for comparison.



187
 188 **Figure S14.** Comparisons of VOCs measured by CHARON-PTR-ToF-MS and Vocus-PTR-ToF-
 189 MS: (a) ketones including methyl vinyl ketone + methacrolein (MVK+MACR), butanone,
 190 pentanone and (b) acids including acetic acid, propionic acid, butyric acid. The Vocus-PTR-ToF-
 191 MS data was scaled for comparison.

192



193
 194 **Figure S15.** Correlation between gaseous $C_5H_{11}O^+$ and $C_5H_9^+$ measured by (a) CHARON-PTR-
 195 ToF-MS and (b) Vocus-PTR-ToF-MS.

196

Table S1. Overview of instruments deployed in the measurement container.

Measured parameters	Instruments	Measurement period
Meteorological parameters	WS700 (Lufft GmbH)	06/05-06/30, 2020
O ₃	Cranox II (Eco Physics®)	06/10-06/30, 2020
CO, CO ₂ , CH ₄ , H ₂ O	CRDS (G2401, Picarro Inc.)	06/10-06/30, 2020
Particle number concentration (> 2.5 nm)	CPC3776 (TSI Inc.)	06/05-06/12, 2020
Particle size distribution (10-410 nm)	NanoScan SMPS3910 (TSI Inc.)	06/05-06/30, 2020
Black carbon (BC)	MA200 (AethLabs Inc.)	06/05-06/30, 2020
Particle concentration (PM _{2.5} and PM ₁₀)	Fidas200 (Palas GmbH)	06/05-06/30, 2020
VOCs and semi-volatile particles	CHARON-PTR-ToF-MS (IONICON GmbH)	06/05-06/30, 2020
VOCs and oxygenated VOCs	Vocus-PTR-ToF-MS (Aerodyne Research Inc.)	06/10-06/30, 2020

197

Table S2. Compositions of gas standard for the calibrations of CHARON-PTR-ToF-MS and Vocus-PTR-ToF-MS.

IONICON certificated gas standard		FZJ home-made gas standard	
Components	Conc. (ppb)	Components	Conc. (ppb)
methanol	98.5 ± 9.1	methanol	867.7 ± 61.7
acetone	98.0 ± 9.1	acetonitrile	865.4 ± 61.5
isoprene	103.0 ± 9.5	acetaldehyde	1229.3 ± 87.4
benzene	94.0 ± 8.7	isoprene	815.5 ± 58.0
toluene	97.0 ± 9.0	benzene	946.7 ± 67.3
o-xylene	102.0 ± 9.4	toluene	945.4 ± 67.2
p-xylene	98.3 ± 9.1	o-xylene	946.3 ± 67.3
m-xylene	94.1 ± 8.8	chlorobenzene	962.8 ± 68.4
1,3,5-trimethylbenzene	108.0 ± 9.9	α-pinene	845.5 ± 60.1
α-pinene	101.0 ± 9.3	1-butanol	859.8 ± 61.1
limonene	95.0 ± 8.8	acetone	1181.5 ± 84.0
		2-butanone	1026.4 ± 73.0
		3-pentanone	1045.1 ± 74.3
		methyl vinyl ketone	1018.4 ± 72.4
		(1R)-(+)-norpinone	502.9 ± 35.8

Table S3. List of 157 VOC ions measured by the Vocus-PTR-ToF-MS included for the PMF analysis

VOC Ion mass (m/z)	Ion formula	Suggested compounds	Averaged mixing ratio (ppb)	Standard deviation
41.039	C ₃ H ₅ ⁺	fragment	0.1852	0.4618
42.034	C ₂ H ₄ N ⁺	acetonitrile	0.0402	0.0213
43.018	C ₂ H ₃ O ⁺	fragment	0.3649	0.2289
43.054	C ₃ H ₇ ⁺	fragment	0.2127	0.5983
47.049	C ₂ H ₇ O ⁺	ethanol	0.2840	0.3444
53.002	C ₃ HO ⁺	unknown	0.0252	0.0379
53.039	C ₄ H ₅ ⁺	fragment	0.0092	0.0076
57.033	C ₃ H ₅ O ⁺	acrolein	0.1823	0.2125
58.041	C ₃ H ₆ O ⁺	acetone charged transfer	0.0030	0.0019
59.049	C ₃ H ₇ O ⁺	acetone	2.0768	0.7845
61.028	C ₂ H ₅ O ₂ ⁺	acetic acid	1.1125	0.6110
63.023	C ₅ H ₃ ⁺	unknown	0.0113	0.0150
65.023	CH ₅ O ₃ ⁺	unknown	0.0011	0.0009
66.046	C ₅ H ₆ ⁺	C ₅ H ₇ charged transfer	0.0015	0.0019
67.054	C ₅ H ₇ ⁺	fragment	0.0282	0.0234
68.062	C ₅ H ₈ ⁺	C ₅ H ₉ charged transfer	0.0019	0.0024
69.033	C ₄ H ₅ O ⁺	furan	0.0097	0.0062
69.07	C ₅ H ₉ ⁺	isoprene	0.4223	0.3694
70.041	C ₄ H ₆ O ⁺	C ₄ H ₇ O charged transfer	0.0006	0.0004
71.049	C ₄ H ₇ O ⁺	MVK/methacrolein	0.1870	0.1122
73.028	C ₃ H ₅ O ₂ ⁺	methyl glyoxal/acrylic acid	0.0467	0.0430
73.065	C ₄ H ₉ O ⁺	MEK/butanal	0.2158	0.1518
75.044	C ₃ H ₇ O ₂ ⁺	acetone water cluster	0.2679	0.1299
77.023	C ₂ H ₅ O ₃ ⁺	glycolic acid	0.0172	0.0167
77.06	C ₃ H ₉ O ₂ ⁺	ethylene glycol	0.5114	0.1969
79.039	C ₂ H ₇ O ₃ ⁺	acetic acid cluster	0.4875	0.3103
79.054	C ₆ H ₇ ⁺	benzene	0.0889	0.0788
81.07	C ₆ H ₉ ⁺	monoterpene fragment	0.4589	0.6799
83.049	C ₅ H ₇ O ⁺	methyl furan	0.0323	0.0176
83.086	C ₆ H ₁₁ ⁺	fragment	0.0503	0.0488
85.028	C ₄ H ₅ O ₂ ⁺	furanone/hydroxy furan	0.0217	0.0141
85.065	C ₅ H ₉ O ⁺	methylcyclopentane	0.0322	0.0161
86.073	C ₅ H ₁₀ O ⁺	C ₅ H ₁₁ O charged transfer	0.0004	0.0002
87.044	C ₄ H ₇ O ₂ ⁺	2,3-butanedione/butyrolactone	0.1783	0.1107
87.08	C ₅ H ₁₁ O ⁺	pentanal/pentanone/3-methylbutanal/allyl ethyl ether	0.0399	0.0490
89.06	C ₄ H ₉ O ₂ ⁺	ethyl acetate/butanoic acid	0.2904	0.2370
91.039	C ₃ H ₇ O ₃ ⁺	lactic acid	0.0260	0.0144
91.054	C ₇ H ₇ ⁺	fragment	0.0171	0.0152
91.075	C ₄ H ₁₁ O ₂ ⁺	water cluster of C ₄ H ₉ O	0.0645	0.0732
92.062	C ₇ H ₈ ⁺	toluene charged transfer	0.0060	0.0068

93.018	C ₂ H ₅ O ₄ ⁺	unknown	0.0008	0.0007
93.055	C ₃ H ₉ O ₃ ⁺	propionic acid water cluster	0.0363	0.0170
93.07	C ₇ H ₉ ⁺	toluene	0.1096	0.0742
95.034	C ₂ H ₇ O ₄ ⁺	unknown	0.0074	0.0058
95.049	C ₆ H ₇ O ⁺	phenol	0.0747	0.0581
95.086	C ₇ H ₁₁ ⁺	monoterpene fragment	0.0364	0.0420
97.028	C ₅ H ₅ O ₂ ⁺	furfural	0.0276	0.0195
97.065	C ₆ H ₉ O ⁺	2-ethylfuran/2,5-dimethylfuran	0.0166	0.0073
97.101	C ₇ H ₁₃ ⁺	fragment	0.0116	0.0142
99.044	C ₅ H ₇ O ₂ ⁺	furfuryl alcohol	0.0537	0.0329
99.08	C ₆ H ₁₁ O ⁺	cyclohexanone	0.0293	0.0173
101.06	C ₅ H ₉ O ₂ ⁺	methyl methacrylate	0.0971	0.0551
101.096	C ₆ H ₁₃ O ⁺	hexanals/hexanones	0.0177	0.0105
103.039	C ₄ H ₇ O ₃ ⁺	acetic anhydride	0.0328	0.0169
103.075	C ₅ H ₁₁ O ₂ ⁺	butanonate	0.0177	0.0092
105.033	C ₇ H ₅ O ⁺	C ₇ 1-oxy 6 DBE	0.0030	0.0023
105.055	C ₄ H ₉ O ₃ ⁺	multiple	0.0295	0.0166
105.091	C ₅ H ₁₃ O ₂ ⁺	1,5-pentanediol	0.0190	0.0140
106.078	C ₈ H ₁₀ ⁺	C ₈ aromatic charged transfer	0.0010	0.0008
107.086	C ₈ H ₁₁ ⁺	C ₈ aromatics	0.0523	0.0411
109.065	C ₇ H ₉ O ⁺	cresol	0.0101	0.0075
109.101	C ₈ H ₁₃ ⁺	terpene fragment	0.0139	0.0249
111.044	C ₆ H ₇ O ₂ ⁺	catechol/benzene diol	0.0406	0.0319
111.08	C ₇ H ₁₁ O ⁺	multiple	0.0149	0.0111
113.023	C ₅ H ₅ O ₃ ⁺	unknown	0.0188	0.0131
113.06	C ₆ H ₉ O ₂ ⁺	unknown	0.0214	0.0108
113.096	C ₇ H ₁₃ O ⁺	ethyl cyclopentanone/	0.0081	0.0049
115.039	C ₅ H ₇ O ₃ ⁺	C ₅ 3-oxy 3D BE	0.0127	0.0090
115.075	C ₆ H ₁₁ O ₂ ⁺	C ₆ diketone isomers/vinylethyl acetate	0.0338	0.0188
115.112	C ₇ H ₁₅ O ⁺	dimethylpentanone/heptanone	0.0066	0.0050
117.055	C ₅ H ₉ O ₃ ⁺	C ₅ 3-oxy 2D BE isomers	0.0350	0.0148
117.091	C ₆ H ₁₃ O ₂ ⁺	ethyl butyrate	0.0171	0.0158
119.034	C ₄ H ₇ O ₄ ⁺	succinic acid	0.1406	0.1318
121.101	C ₉ H ₁₃ ⁺	C ₉ aromatics	0.0343	0.0286
123.044	C ₇ H ₇ O ₂ ⁺	benzoic acid	0.0151	0.0101
123.08	C ₈ H ₁₁ O ⁺	methylanisole	0.0030	0.0015
123.117	C ₉ H ₁₅ ⁺	terpene fragment	0.0086	0.0052
125.096	C ₈ H ₁₃ O ⁺	C ₄ substituted furan	0.0080	0.0043
129.091	C ₇ H ₁₃ O ₂ ⁺	allyl ester isobutyric acid	0.0166	0.0091
129.127	C ₈ H ₁₇ O ⁺	octanal	0.0146	0.0120
131.034	C ₅ H ₇ O ₄ ⁺	isoprene oxidation product	0.0127	0.0074
131.07	C ₆ H ₁₁ O ₃ ⁺	multiple	0.0169	0.0124
131.107	C ₇ H ₁₅ O ₂ ⁺	C ₇ carboxylic acid	0.0045	0.0023

133.05	C ₅ H ₉ O ₄ ⁺	glutaric acid	0.0160	0.0096
133.101	C ₁₀ H ₁₃ ⁺	multiple	0.0056	0.0045
136.125	C ₁₀ H ₁₆ ⁺	monoterpene charged transfer	0.0039	0.0057
137.132	C ₁₀ H ₁₇ ⁺	monoterpenes	0.8682	1.4585
139.075	C ₈ H ₁₁ O ₂ ⁺	2-methoxy-4-methylphenol	0.0040	0.0028
139.112	C ₉ H ₁₅ O ⁺	monoterpene oxidation product (e.g., nopinone)	0.0527	0.0368
141.055	C ₇ H ₉ O ₃ ⁺	methoxycatechol	0.0066	0.0033
141.091	C ₈ H ₁₃ O ₂ ⁺	unknown	0.0075	0.0044
141.127	C ₉ H ₁₇ O ⁺	trans-2-nonenal	0.0056	0.0029
143.07	C ₇ H ₁₁ O ₃ ⁺	unknown	0.0062	0.0036
143.107	C ₈ H ₁₅ O ₂ ⁺	unknown	0.0128	0.0101
143.143	C ₉ H ₁₉ O ⁺	nonanal/2-nonanone	0.0341	0.0299
145.086	C ₇ H ₁₃ O ₃ ⁺	unknown	0.0058	0.0029
145.122	C ₈ H ₁₇ O ₂ ⁺	ethyl hexanoate	0.0033	0.0018
147.065	C ₆ H ₁₁ O ₄ ⁺	unknown	0.0072	0.0042
149.023	C ₈ H ₅ O ₃ ⁺	phthalic anhydride	0.0019	0.0018
149.096	C ₁₀ H ₁₃ O ⁺	unknown	0.0034	0.0030
149.132	C ₁₁ H ₁₇ ⁺	sesquiterpene fragment	0.0013	0.0011
151.075	C ₉ H ₁₁ O ₂ ⁺	vinyl guaiacol/benzyl acetate	0.0015	0.0009
151.112	C ₁₀ H ₁₅ O ⁺	monoterpene oxidation product (e.g., pinonaldehyde fragment)	0.0244	0.0165
153.055	C ₈ H ₉ O ₃ ⁺	methyl salicylate	0.0179	0.0081
153.091	C ₉ H ₁₃ O ₂ ⁺	unknown	0.0050	0.0027
153.127	C ₁₀ H ₁₇ O ⁺	camphor/monoterpene oxidation product	0.0230	0.0150
155.07	C ₈ H ₁₁ O ₃ ⁺	syringol	0.0025	0.0016
155.107	C ₉ H ₁₅ O ₂ ⁺	monoterpene oxidation product	0.0060	0.0044
155.143	C ₁₀ H ₁₉ O ⁺	linalool	0.0091	0.0130
157.086	C ₈ H ₁₃ O ₃ ⁺	monoterpene oxidation product (e.g., terpenylic acid)	0.0057	0.0032
157.122	C ₉ H ₁₇ O ₂ ⁺	C ₉ 2-oxy 2DBE isomers	0.0110	0.0064
157.159	C ₁₀ H ₂₁ O ⁺	menthol-type monoterpenes/ decanal	0.0189	0.0471
159.065	C ₇ H ₁₁ O ₄ ⁺	3,6-oxoheptanoic acid	0.0045	0.0024
159.102	C ₈ H ₁₅ O ₃ ⁺	monoterpene oxidation product	0.0046	0.0036
159.138	C ₉ H ₁₉ O ₂ ⁺	methyl octanoate	0.0027	0.0015
161.081	C ₇ H ₁₃ O ₄ ⁺	unknown	0.0032	0.0019
165.055	C ₉ H ₉ O ₃ ⁺	unknown	0.0007	0.0006
167.034	C ₈ H ₇ O ₄ ⁺	terephthalic acid	0.0047	0.0034
167.107	C ₁₀ H ₁₅ O ₂ ⁺	monoterpene oxidation product	0.0063	0.0033
169.05	C ₈ H ₉ O ₄ ⁺	C ₈ 4-oxy 5-DBE	0.0006	0.0005
169.086	C ₉ H ₁₃ O ₃ ⁺	C ₉ 3-oxy 4-DBE	0.0021	0.0013
169.122	C ₁₀ H ₁₇ O ₂ ⁺	monoterpene oxidation product (e.g. pinonaldehyde)	0.0216	0.0160
171.029	C ₇ H ₇ O ₅ ⁺	unknown	0.0014	0.0011
171.065	C ₈ H ₁₁ O ₄ ⁺	unknown	0.0012	0.0006

171.102	C ₉ H ₁₅ O ₃ ⁺	monoterpene oxidation product	0.0048	0.0024
171.138	C ₁₀ H ₁₉ O ₂ ⁺	linalool oxide	0.0066	0.0040
173.044	C ₇ H ₉ O ₅ ⁺	toluene oxidation product	0.0007	0.0005
173.081	C ₈ H ₁₃ O ₄ ⁺	monoterpene oxidation product	0.0020	0.0013
173.117	C ₉ H ₁₇ O ₃ ⁺	unknown	0.0014	0.0016
173.154	C ₁₀ H ₂₁ O ₂ ⁺	unknown	0.0016	0.0011
175.06	C ₇ H ₁₁ O ₅ ⁺	unknown	0.0024	0.0013
175.096	C ₈ H ₁₅ O ₄ ⁺	monoterpene oxidation product	0.0014	0.0009
183.102	C ₁₀ H ₁₅ O ₃ ⁺	monoterpene oxidation product	0.0026	0.0014
185.117	C ₁₀ H ₁₇ O ₃ ⁺	monoterpene oxidation product (e.g., <i>cis</i> -pinonic acid)	0.0066	0.0037
185.154	C ₁₁ H ₂₁ O ₂ ⁺	unknown	0.0007	0.0004
187.096	C ₉ H ₁₅ O ₄ ⁺	monoterpene oxidation product (e.g., pinic acid)	0.0018	0.0009
189.076	C ₈ H ₁₃ O ₅ ⁺	monoterpene oxidation product	0.0009	0.0005
189.149	C ₁₀ H ₂₁ O ₃ ⁺	unknown	0.0002	0.0002
193.159	C ₁₃ H ₂₁ O ⁺	unknown	0.0004	0.0010
195.138	C ₁₂ H ₁₉ O ₂ ⁺	unknown	0.0004	0.0002
197.081	C ₁₀ H ₁₃ O ₄ ⁺	unknown	0.0003	0.0002
197.117	C ₁₁ H ₁₇ O ₃ ⁺	unknown	0.0004	0.0002
197.154	C ₁₂ H ₂₁ O ₂ ⁺	unknown	0.0002	0.0002
199.096	C ₁₀ H ₁₅ O ₄ ⁺	monoterpene oxidation product	0.0010	0.0005
199.133	C ₁₁ H ₁₉ O ₃ ⁺	unknown	0.0007	0.0003
201.112	C ₁₀ H ₁₇ O ₄ ⁺	monoterpene oxidation product	0.0011	0.0006
203.091	C ₉ H ₁₅ O ₅ ⁺	monoterpene oxidation product	0.0004	0.0003
203.128	C ₁₀ H ₁₉ O ₄ ⁺	unknown	0.0002	0.0002
205.071	C ₈ H ₁₃ O ₆ ⁺	monoterpene oxidation product	0.0003	0.0002
205.195	C ₁₅ H ₂₅ ⁺	sesquiterpenes	0.0039	0.0037
209.154	C ₁₃ H ₂₁ O ₂ ⁺	unknown	0.0004	0.0003
213.076	C ₁₀ H ₁₃ O ₅ ⁺	monoterpene oxidation product	0.0002	0.0001
215.091	C ₁₀ H ₁₅ O ₅ ⁺	monoterpene oxidation product	0.0003	0.0002
215.128	C ₁₁ H ₁₉ O ₄ ⁺	unknown	0.0002	0.0002
217.107	C ₁₀ H ₁₇ O ₅ ⁺	monoterpene oxidation product	0.0003	0.0001
217.143	C ₁₁ H ₂₁ O ₄ ⁺	unknown	0.0001	0.0001
223.169	C ₁₄ H ₂₃ O ₂ ⁺	sesquiterpene oxidation product	0.0003	0.0011

Table S4. Comparison of 112 VOC ions measured by Vocus-PTR-ToF-MS to those measured by CHARON-PTR-ToF-MS during second measurement period (22nd-30th June 2020).

No.	VOC ions	Pearson's r	Slope	Intercept	No.	VOC ions	Pearson's r	Slope	Intercept
1	C ₃ H ₅ ⁺	0.10	0.002	0.097	57	C ₇ H ₁₃ O ₂ ⁺	0.86	2.170	0.002
2	C ₃ H ₇ ⁺	0.08	0.004	0.077	58	C ₈ H ₁₇ O ⁺	0.01	0.119	0.012
3	C ₂ H ₇ O ⁺	0.74	4.405	0.083	59	C ₅ H ₇ O ₄ ⁺	0.67	3.582	-0.008
4	C ₄ H ₅ ⁺	0.38	0.038	0.011	60	C ₆ H ₁₁ O ₃ ⁺	0.11	2.379	0.013
5	C ₃ H ₇ O ⁺	0.82	0.429	0.030	61	C ₇ H ₁₅ O ₂ ⁺	0.65	2.148	0.004
6	C ₂ H ₅ O ₂ ⁺	0.81	0.849	-0.164	62	C ₅ H ₉ O ₄ ⁺	0.18	1.535	0.017
7	CH ₅ O ₃ ⁺	-0.31	-0.036	0.001	63	C ₁₀ H ₁₃ ⁺	0.54	0.307	0.003
8	C ₅ H ₇ ⁺	0.41	0.110	0.019	64	C ₁₀ H ₁₇ ⁺	0.59	0.559	0.252
9	C ₄ H ₅ O ⁺	0.39	0.205	0.004	65	C ₈ H ₁₁ O ₂ ⁺	0.41	0.239	0.003
10	C ₅ H ₉ ⁺	0.92	1.652	0.025	66	C ₉ H ₁₅ O ⁺	0.93	2.903	0.001
11	C ₄ H ₇ O ⁺	0.94	1.292	-0.002	67	C ₇ H ₉ O ₃ ⁺	0.69	0.543	0.001
12	C ₃ H ₅ O ₂ ⁺	0.75	0.775	-0.021	68	C ₈ H ₁₃ O ₂ ⁺	0.76	1.004	0.003
13	C ₄ H ₉ O ⁺	0.96	2.256	-0.053	69	C ₉ H ₁₇ O ⁺	0.55	2.281	0.000
14	C ₃ H ₇ O ₂ ⁺	0.89	2.842	-0.001	70	C ₇ H ₁₁ O ₃ ⁺	0.73	1.841	0.001
15	C ₃ H ₉ O ₂ ⁺	0.50	16.469	0.185	71	C ₈ H ₁₅ O ₂ ⁺	0.17	1.030	0.008
16	C ₆ H ₇ ⁺	0.33	0.313	0.079	72	C ₉ H ₁₉ O ⁺	0.20	22.151	0.021
17	C ₆ H ₉ ⁺	0.55	0.201	0.188	73	C ₇ H ₁₃ O ₃ ⁺	0.68	5.837	0.005
18	C ₅ H ₇ O ⁺	0.82	0.987	0.002	74	C ₈ H ₁₇ O ₂ ⁺	0.53	1.393	0.005
19	C ₆ H ₁₁ ⁺	0.21	0.910	0.039	75	C ₆ H ₁₁ O ₄ ⁺	0.54	3.029	0.003
20	C ₄ H ₅ O ₂ ⁺	0.71	0.629	-0.004	76	C ₈ H ₅ O ₃ ⁺	0.72	0.256	0.001
21	C ₅ H ₉ O ⁺	0.82	1.702	0.004	77	C ₁₀ H ₁₃ O ⁺	0.76	0.627	-0.001
22	C ₄ H ₇ O ₂ ⁺	0.72	4.300	-0.051	78	C ₁₁ H ₁₇ ⁺	0.37	0.311	0.002
23	C ₅ H ₁₁ O ⁺	0.44	3.108	0.005	79	C ₉ H ₁₁ O ₂ ⁺	0.48	0.254	0.001
24	C ₄ H ₉ O ₂ ⁺	0.66	17.104	-0.112	80	C ₁₀ H ₁₅ O ⁺	0.87	1.911	0.006
25	C ₃ H ₇ O ₃ ⁺	0.23	0.347	0.023	81	C ₈ H ₉ O ₃ ⁺	0.85	1.025	0.004
26	C ₄ H ₁₁ O ₂ ⁺	0.77	15.001	-0.273	82	C ₉ H ₁₃ O ₂ ⁺	-0.04	-0.048	0.006
27	C ₇ H ₉ ⁺	0.66	0.499	0.056	83	C ₁₀ H ₁₇ O ⁺	0.85	1.374	0.003
28	C ₆ H ₇ O ⁺	0.50	3.027	-0.045	84	C ₈ H ₁₁ O ₃ ⁺	0.88	0.355	0.000
29	C ₇ H ₁₁ ⁺	0.45	0.103	0.023	85	C ₉ H ₁₅ O ₂ ⁺	0.37	1.035	0.006
30	C ₅ H ₅ O ₂ ⁺	0.53	0.967	-0.005	86	C ₁₀ H ₁₉ O ⁺	0.05	0.506	0.003
31	C ₆ H ₉ O ⁺	0.77	0.405	0.005	87	C ₈ H ₁₃ O ₃ ⁺	0.46	2.795	0.005

32	C ₇ H ₁₃ ⁺	0.07	0.220	0.015	88	C ₉ H ₁₇ O ₂ ⁺	0.62	2.958	0.003
33	C ₅ H ₇ O ₂ ⁺	0.62	1.275	-0.001	89	C ₁₀ H ₂₁ O ⁺	0.11	25.598	0.019
34	C ₆ H ₁₁ O ⁺	0.91	3.464	0.001	90	C ₇ H ₁₁ O ₄ ⁺	0.81	2.565	-0.001
35	C ₅ H ₉ O ₂ ⁺	0.52	1.931	0.039	91	C ₉ H ₉ O ₃ ⁺	0.53	0.327	0.000
36	C ₆ H ₁₃ O ⁺	0.77	6.056	-0.003	92	C ₈ H ₇ O ₄ ⁺	0.64	3.022	-0.003
37	C ₄ H ₇ O ₃ ⁺	0.80	4.988	-0.008	93	C ₁₀ H ₁₅ O ₂ ⁺	0.79	1.203	0.001
38	C ₅ H ₁₁ O ₂ ⁺	0.71	2.424	0.009	94	C ₈ H ₉ O ₄ ⁺	0.53	0.147	0.000
39	C ₈ H ₁₁ ⁺	0.85	0.861	0.016	95	C ₉ H ₁₃ O ₃ ⁺	0.67	0.543	0.001
40	C ₇ H ₉ O ₁ ⁺	0.50	0.664	0.006	96	C ₁₀ H ₁₇ O ₂ ⁺	0.57	8.491	-0.004
41	C ₈ H ₁₃ ⁺	0.10	0.172	0.015	97	C ₇ H ₇ O ₅ ⁺	0.17	0.367	0.002
42	C ₆ H ₇ O ₂ ⁺	0.64	2.227	-0.010	98	C ₈ H ₁₁ O ₄ ⁺	0.69	0.132	0.000
43	C ₇ H ₁₁ O ⁺	0.85	1.352	0.000	99	C ₉ H ₁₅ O ₃ ⁺	0.57	1.675	0.005
44	C ₅ H ₅ O ₃ ⁺	0.74	0.843	0.002	100	C ₇ H ₉ O ₅ ⁺	0.39	0.274	0.000
45	C ₆ H ₉ O ₂ ⁺	0.88	1.172	-0.004	101	C ₈ H ₁₃ O ₄ ⁺	0.74	0.982	0.000
46	C ₇ H ₁₃ O ⁺	0.89	3.037	0.003	102	C ₁₀ H ₂₁ O ₂ ⁺	0.23	0.208	0.002
47	C ₅ H ₇ O ₃ ⁺	0.26	0.381	0.004	103	C ₇ H ₁₁ O ₅ ⁺	0.71	1.546	0.001
48	C ₆ H ₁₁ O ₂ ⁺	0.91	2.246	-0.001	104	C ₈ H ₁₅ O ₄ ⁺	0.37	1.602	0.001
49	C ₇ H ₁₅ O ⁺	0.63	3.979	0.001	105	C ₁₀ H ₁₅ O ₃ ⁺	0.72	0.867	0.000
50	C ₅ H ₉ O ₃ ⁺	0.70	8.684	0.004	106	C ₁₀ H ₁₇ O ₃ ⁺	0.23	0.819	0.006
51	C ₆ H ₁₃ O ₂ ⁺	0.42	4.490	0.015	107	C ₉ H ₁₅ O ₄ ⁺	0.48	0.607	0.001
52	C ₉ H ₁₃ ⁺	0.82	0.826	0.008	108	C ₈ H ₁₃ O ₅ ⁺	0.77	0.589	0.000
53	C ₇ H ₇ O ₂ ⁺	0.61	0.982	0.003	109	C ₁₀ H ₁₃ O ₄ ⁺	0.37	0.071	0.000
54	C ₈ H ₁₁ O ⁺	0.73	0.387	0.001	110	C ₁₀ H ₁₅ O ₄ ⁺	0.53	0.097	0.000
55	C ₉ H ₁₅ ⁺	0.66	0.583	0.004	111	C ₁₅ H ₂₅ ⁺	0.71	0.554	-0.001
56	C ₈ H ₁₃ O ⁺	0.59	0.910	0.003	112	C ₁₀ H ₁₅ O ₅ ⁺	0.87	0.147	0.002

200 The Pearson's r was >0.5 in bold.

201 **References**

- 202 Bosque, R. and Sales, J.: Polarizabilities of Solvents from the Chemical Composition, *Journal of*
203 *Chemical Information and Computer Sciences*, 42, 1154-1163, 10.1021/ci025528x, 2002.
- 204 Coggon, M. M., Stockwell, C. E., Xu, L., Peischl, J., Gilman, J. B., Lamplugh, A., Bowman, H. J.,
205 Aikin, K., Harkins, C., Zhu, Q., Schwantes, R. H., He, J., Li, M., Seltzer, K., McDonald,
206 B., and Warneke, C.: Contribution of cooking emissions to the urban volatile organic
207 compounds in Las Vegas, NV, *Atmos. Chem. Phys.*, 24, 4289-4304, 10.5194/acp-24-4289-
208 2024, 2024.
- 209 Gioumousis, G. and Stevenson, D. P.: Reactions of Gaseous Molecule Ions with Gaseous
210 Molecules. V. Theory, *The Journal of Chemical Physics*, 29, 294-299, 10.1063/1.1744477,
211 1958.
- 212 Karl, T., Hansel, A., Cappellin, L., Kaser, L., Herdlinger-Blatt, I., and Jud, W.: Selective
213 measurements of isoprene and 2-methyl-3-buten-2-ol based on NO⁺
214 ionization mass spectrometry, *Atmos. Chem. Phys.*, 12, 11877-11884, 10.5194/acp-12-
215 11877-2012, 2012.
- 216 Leglise, J., Müller, M., Piel, F., Otto, T., and Wisthaler, A.: Bulk Organic Aerosol Analysis by
217 Proton-Transfer-Reaction Mass Spectrometry: An Improved Methodology for the
218 Determination of Total Organic Mass, O:C and H:C Elemental Ratios, and the Average
219 Molecular Formula, *Anal. Chem.*, 91, 12619-12624, 10.1021/acs.analchem.9b02949, 2019.
- 220 Müller, M., Eichler, P., D'Anna, B., Tan, W., and Wisthaler, A.: Direct Sampling and Analysis of
221 Atmospheric Particulate Organic Matter by Proton-Transfer-Reaction Mass Spectrometry,
222 *Anal. Chem.*, 89, 10889-10897, 10.1021/acs.analchem.7b02582, 2017.
- 223 Pfannerstill, E. Y., Arata, C., Zhu, Q., Schulze, B. C., Woods, R., Seinfeld, J. H., Bucholtz, A.,
224 Cohen, R. C., and Goldstein, A. H.: Volatile organic compound fluxes in the agricultural
225 San Joaquin Valley – spatial distribution, source attribution, and inventory comparison,
226 *Atmos. Chem. Phys.*, 23, 12753-12780, 10.5194/acp-23-12753-2023, 2023.
- 227 Piel, F., Müller, M., Winkler, K., Skytte af Sättra, J., and Wisthaler, A.: Introducing the extended
228 volatility range proton-transfer-reaction mass spectrometer (EVR PTR-MS), *Atmos. Meas.*
229 *Tech.*, 14, 1355-1363, 10.5194/amt-14-1355-2021, 2021.
- 230 Su, T. and Chesnavich, W. J.: Parametrization of the ion–polar molecule collision rate constant by
231 trajectory calculations, *The Journal of Chemical Physics*, 76, 5183-5185, 10.1063/1.442828,
232 1982.
- 233 Yuan, B., Koss, A. R., Warneke, C., Coggon, M., Sekimoto, K., and de Gouw, J. A.: Proton-
234 Transfer-Reaction Mass Spectrometry: Applications in Atmospheric Sciences, *Chemical*
235 *Reviews*, 117, 13187-13229, 10.1021/acs.chemrev.7b00325, 2017.

236